Transverse and longitudinal electromagnetic modes in metallic superlattices

Hua Shi and Allan Griffin
Department of Physics, University of Toronto, Toronto, Ontario, Canada M5S 1A7
(Received 10 June 1991)

We give a simple unified analysis of the longitudinal and transverse plasmons in a superlattice of metallic sheets. We evaluate the longitudinal and transverse conductivities in the random-phase approximation in a momentum-space formalism closely patterned after the standard approach used in bulk metals. A detailed analysis is presented (with retardation fully included) of how the longitudinal and transverse plasmon frequencies depend on the sheet separation d. The photon line $\omega = ck_{\|}$ separates the two kinds of superlattice modes, with the exception of the $k_z = 0$ longitudinal plasmon.

I. INTRODUCTION

A superlattice is a periodic array of metallic sheets in which there is negligible charge transfer (it is often referred to as a layered electron gas or LEG). There is a considerable literature on the longitudinal plasmon spectrum of a superlattice (see, for example, Refs. 1–3). In addition, the propagation of electromagnetic waves and how they couple to charge fluctuations have been discussed (see, for example, Refs. 4–6). The older literature on collective modes in superlattices was motivated by experiments on epitaxially grown layered semiconductors. In this case, the number of conducting layers is usually quite small and surface-interface effects are of considerable interest. Moreover the layers have finite thickness and thus are best described as quantum wells with an associated electronic state spectrum. The recent literature on collective modes in semiconductor superlattice has put emphasis on including such multiple subbands (see,for example, Ref. 6). In the limit of thick enough layers, one can treat the superlattice as a periodic array of layers each described by a bulk dielectric function (see, for example, Ref. 7). More recently, the theory of infinite metallic superlattices has found a new application in the study of the new high-T_c superconductors. These may be viewed as a periodic array of unit cells (with a typical spacing of about 12 Å), each of which contains up to three closely spaced CuO_2 sheets. Even at these small separations, the electronic bands are 2D-like, showing that there is almost no charge transfer or tunneling between the sheets. In this case, the metallic layers really are truly two-dimensional (2D). For further discussion of the high-T_c superconductors as infinite metallic superlattices, see Ref. 8. This system is the motivation of the present work.

The main purpose of this paper is to give a simple, self-contained, unified analysis of both the longitudinal and transverse plasmon modes in a metallic superlattice, including the effects of retardation on the former. Our analysis should be especially useful for readers who are not experts in the layered electron gas literature as applied to semiconductors. While we discuss superlattices without a basis, it is straightforward to extend the analysis of the paper to deal with the longitudinal and transverse modes in a superlattice with several closely spaced sheets in each unit cell. In Sec. VI, we illustrate this by working out the effects of retardation on the well known longitudinal plasmons of a two layer (bilayer) system.

Our formal derivation of the dispersion relations is most similar to that of Refs. 4 and 6. However, in contrast to previous studies, we formulate the problem (in momentum space) in terms of calculating the longitudinal and transverse conductivities of the superlattice within the random-phase approximation (RPA). We try to present our analysis in a form analogous to the usual momentum-space treatment of longitudinal and transverse modes in bulk metals (see, for example, Pines and Nozières[9] and Martin[10]), modified to take into account the periodic structure. In our momentum-space formulation, the periodicity is most naturally described using the reciprocal lattice vectors of the (1D) superlattice. We believe that our approach brings out the physics involved in both kinds of mode in a clear fashion and also gives a formalism which can be generalized to deal with more than one metallic sheet per unit cell.

We also give a detailed examination and comparison of how the longitudinal plasmons (including retardation) and transverse plasmons depend on the spacing d between the sheets. Most explicit discussions of the longitudinal plasmons in the literature have emphasized the nonretarded ($c \to \infty$ or electrostatic) limit. We are not aware of any similar analysis in the literature as is given in Secs. III–V. Quinn and co-workers (Refs. 4, 5, and 11) worked out the special case when there is a large magnetic field perpendicular to the sheets. King-Smith and Inkson[6] only considered the $k_{\|}d, k_z d \ll 1$ limits. The dependence of the superlattice plasmon spectrum on the spacing d is found to be surprisingly delicate. The longitudinal plasmons are restricted to the frequency region $\omega < ck_{\|}$, with the exception of the $k_z = 0$ mode where all sheets oscillate in phase. The transverse plasmons are restricted to the region $\omega > ck_{\|}$ and do not exist in the limit $d \to \infty$ (i.e., there are no transverse plasmons associated with a single sheet).

In Sec. II, we combine Maxwell's equations with linear

response theory (following Harris and Griffin[12]) and write down the general self-consistent integral equations for the conductivity tensor $\sigma_{ij}(\mathbf{k},-\mathbf{p},\omega)$. We then specialize these equations to a periodic array of metallic sheets and work out the transverse and longitudinal conductivities within the RPA. In this approach, the collective modes arise as poles of the appropriate conductivities. The formal dispersion relations are given in terms of the longitudinal $\sigma_l^0(\mathbf{k}_\parallel,\omega)$ and transverse $\sigma_t^0(\mathbf{k}_\parallel,\omega)$ conductivities of a noninteracting 2D electron gas and a universal function $R(\mathbf{k}_\parallel,k_z,\omega)$ [see Eq. (19)] which contains all effects of the periodic structure. The formal dispersion relations we find reduce to the ones obtained in the literature by a variety of approaches (see, for example, Refs. 1, 4, 6, and 13).

In Secs. III–V, we give a detailed analytic discussion of the solutions of these dispersion relations. We are interested in understanding how the plasmons in a superlattice with spacing d compare with those of 2D and 3D bulk metals. In the limit of large d, the results go over to those of a single sheet. In this case the nonretarded longitudinal 2D plasmon (n_0 is the charge density per unit area)

$$\omega_{2D}=\left[\frac{2\pi n_0 e^2}{m}k_\parallel\right]^{1/2} \tag{1}$$

goes over to $ck_\parallel$ as $k_\parallel\to 0$.[14,15] As we have mentioned, there is no transverse plasmon in a 2D metallic sheet. In the opposite limit of small d, the collective modes go over to those of a 3D metal[9]

$$\begin{aligned}\omega_l&=\left[\frac{4\pi n_B e^2}{m}\right]^{1/2}\equiv\omega_B\ ,\\ \omega_t&=(\omega_B^2+c^2k^2)^{1/2}\ .\end{aligned} \tag{2}$$

In contrast with the 2D plasmon, there is no effect of retardation on the long wavelength 3D longitudinal plasmon.[14]

II. LONGITUDINAL AND TRANSVERSE CONDUCTIVITIES OF A SUPERLATTICE

In this section, we combine Maxwell's equations with linear response theory to derive the self-consistent equations for the induced electric fields and the associated conductivity tensor.[10] Then we specialize the results to the case of a periodic array of 2D metallic sheets and find explicit expressions for the longitudinal and transverse conductivities within the random-phase approximation. The associated collective modes are given by the poles of these conductivities.

Maxwell's equations can be reduced to coupled equations for the components of the induced electric fields and currents,[12]

$$\delta E_i(\mathbf{k},\omega)=\frac{4\pi i}{\omega(\omega^2-c^2k^2)}\sum_j(c^2k_ik_j-\omega^2\delta_{ij})\delta J_j(\mathbf{k},\omega)\ , \tag{3}$$

where

$$A(\mathbf{r},t)\equiv\int\frac{d\mathbf{k}}{(2\pi)^3}\int\frac{d\omega}{2\pi}e^{-i\mathbf{k}\cdot\mathbf{r}+i\omega t}A(\mathbf{k},\omega)\ , \tag{4}$$

and k_i represents the Cartesian component of $\mathbf{k}$ along the ith axis ($i,j=x,y,z$). The total or net electric field is given by $E_i(\mathbf{k},\omega)=E_{\text{ext},i}(\mathbf{k},\omega)+\delta E_i(\mathbf{k},\omega)$. We next introduce the conductivity tensor in the usual way,

$$\delta J_i(\mathbf{k},\omega)=\sum_j\int\frac{d\mathbf{p}}{(2\pi)^3}\sigma_{ij}(\mathbf{k},-\mathbf{p},\omega)E_{\text{ext},j}(\mathbf{p},\omega) \tag{5}$$

$$=\sum_j\int\frac{d\mathbf{p}}{(2\pi)^3}\sigma_{ij}^{sc}(\mathbf{k},-\mathbf{p},\omega)E_j(\mathbf{p},\omega)\ . \tag{6}$$

The result in (6) may be viewed as a definition of the screened conductivity tensor σ_{ij}^{sc} as the response to the true electric field.[10,12] All long-range effects arising from the Coulomb interaction are contained in the true electric field E_i defined above. Combining (6) and (3) gives us an integral equation for the electric field components

$$\begin{aligned}E_i(\mathbf{k},\omega)=&E_{\text{ext},i}(\mathbf{k},\omega)\\&+\frac{4\pi i}{\omega(\omega^2-c^2k^2)}\sum_{j,m}\int\frac{d\mathbf{p}}{(2\pi)^3}(c^2k_ik_j-\omega^2\delta_{ij})\\&\times\sigma_{jm}^{sc}(\mathbf{k},-\mathbf{p},\omega)E_m(\mathbf{p},\omega)\ .\end{aligned} \tag{7}$$

This can be equivalently expressed as an integral equation for the component of the conductivity tensor by using (5) and (6),

$$\begin{aligned}\sigma_{ij}(\mathbf{k},-\mathbf{p},\omega)=&\sigma_{ij}^{sc}(\mathbf{k},-\mathbf{p},\omega)\\&+\sum_{n,m}\int\frac{d\mathbf{q}}{(2\pi)^3}\sigma_{in}^{sc}(\mathbf{k},-\mathbf{q},\omega)\\&\times\frac{4\pi i(c^2q_nq_m-\omega^2\delta_{nm})}{\omega(\omega^2-c^2q^2)}\\&\times\sigma_{mj}(\mathbf{q},-\mathbf{p},\omega)\ .\end{aligned} \tag{8}$$

Equations (7) and (8) are the natural starting point for application to specific systems, which are characterized by our choice for σ_{ij}^{sc}. In general, we have (see for example, Ref. 12)

$$\sigma_{ij}(\mathbf{k},-\mathbf{p},\omega)=\frac{ie^2}{m\omega}n_0(\mathbf{k}-\mathbf{p})\delta_{ij}+\frac{e^2}{i\omega}\chi_{J_iJ_j}(\mathbf{k},-\mathbf{p},\omega)\ , \tag{9}$$

where $n_0(\mathbf{k})$ is the Fourier transform of the electronic charge density and $\chi_{J_iJ_j}\equiv\chi_{ij}$ is the Fourier transform of the current-current correlation function.

While longitudinal collective modes are specifically associated with charge density fluctuations, transverse collective modes can arise in vacuum. These free photon ($\omega=ck$) resonances are evident in (7) and (8). The transverse modes we will be interested in are electromagnetic (EM) waves which couple into the charge fluctuations in the metallic sheets.

We now turn to a periodic array of two-dimensional (2D) metallic sheets (in the x-y plane), the separation dis-

tance being d. In this metallic superlattice, the number and current densities are restricted to the sheets, being given by

$$n_0(\mathbf{r})=n_0\sum_l \delta(z-ld)\ ,$$
$$\mathbf{J}(\mathbf{r})=-en_0\sum_l v_l(\mathbf{r}_\parallel)\delta(z-ld)\ . \tag{10}$$

Here $v_l(\mathbf{r}_\parallel)$ is the velocity of an electron in the lth sheet at some point $\mathbf{r}_\parallel=(x,y)$. We also restrict ourselves to the RPA, which corresponds[9] to approximating σ_{ij}^{sc} by the conductivity tensor σ_{ij}^0 of a *noninteracting* electron gas.

For our superlattice described by (10), one can show that[8] (for $i,j=x,y$)

$$\sigma_{ij}^0(\mathbf{k},-\mathbf{p},\omega)=(2\pi)^2\delta(\mathbf{k}_\parallel-\mathbf{p}_\parallel)\sigma_{ij}^0(\mathbf{k}_\parallel,\omega)N\sum_{G_z}\delta_{p_z,k_z+G_z}\ , \tag{11}$$

where $G_z=n(2\pi/d)$ ($n=0,\pm1,\pm2,\ldots$) are the reciprocal lattice vectors of a 1D lattice and $\sigma_{ij}^0(\mathbf{k}_\parallel,\omega)$ is the conductivity tensor of a 2D free-electron gas. Since currents can only flow in the x-y plane, one finds σ_{ij}^0 vanishes when *either* i or j involves the z component of the current operator.

Taking the above features into account, (7) and (8) simplify considerably for a superlattice. Using (11) and (7), we have for $i=x,y$

$$(\omega^2-c^2k^2)\delta E_i(\mathbf{k}_\parallel,k_z,\omega)=\frac{4\pi i}{\omega}\sum_{n,m=x,y}(c^2k_ik_n-\omega^2\delta_{in})\sigma_{nm}^0(\mathbf{k}_\parallel,\omega)\frac{1}{d}\sum_{G_z}E_m(\mathbf{k}_\parallel,k_z+G_z)\ . \tag{12}$$

We note that (12) gives two closed coupled equations for the in-plane components E_x and E_y. In addition, the z component of the electric field is

$$(\omega^2-c^2k^2)E_z(\mathbf{k}_\parallel,k_z,\omega)=\frac{4\pi i}{\omega}c^2k_z\sum_{n,m=x,y}k_n\sigma_{nm}^0(\mathbf{k}_\parallel,\omega)\frac{1}{d}\sum_{G_z}E_m(\mathbf{k}_\parallel,k_z+G_z)\ . \tag{13}$$

That is, the induced E_z component is completely determined by the solutions E_x and E_y of (12). The results in (12) and (13) form the basis for our further analysis of EM modes in a superlattice.

The conductivity tensor of a homogeneous 2D electron gas can be split into longitudinal and transverse components and hence ($i,j=x,y$)

$$\sigma_{ij}^0=\sigma_l^0\hat{k}_i\hat{k}_j+\sigma_t^0(\delta_{ij}-\hat{k}_i\hat{k}_j)\ , \tag{14}$$

where the in-plane unit vectors are defined as $\hat{k}_i\equiv k_i/k_\parallel$, where $k_\parallel=\sqrt{k_x^2+k_y^2}$. Similarly the in-plane electric field can be split into longitudinal and transverse fields, with

$$E_i^l\equiv\hat{k}_i\sum_{j=x,y}\hat{k}_jE_j\ ,$$
$$E_i^t\equiv E_i-E_i^l=\sum_j(\delta_{ij}-\hat{k}_i\hat{k}_j)E_j\ . \tag{15}$$

One easily verifies that $\mathbf{k}_\parallel\cdot\mathbf{E}_\parallel=\mathbf{k}_\parallel\cdot\mathbf{E}_\parallel^l$ and $\mathbf{k}_\parallel\cdot\mathbf{E}_\parallel^t=0$. Using (14) and (15) in (12), one can show that ($i=x,y$)

$$\delta E_i(k_z)=\frac{-4\pi i}{\omega(\omega^2-c^2k^2)}\times[\sigma_l^0(\omega^2-c^2k_\parallel^2)\bar{E}_i^l(k_z)+\sigma_t^0\omega^2\bar{E}_i^t(k_z)]\ , \tag{16}$$

where we have defined

$$\bar{E}_i^{l,t}(k_z)\equiv\frac{1}{d}\sum_{G_z}E_i^{l,t}(\mathbf{k}_\parallel,k_z+G_z)\ . \tag{17}$$

We first discuss longitudinal modes. Using the fact that $\bar{E}_i^{l,t}(k_z+G_z)=\bar{E}_i^{l,t}(k_z)$, (16) and (17) lead to

$$\delta\bar{E}_i^l(k_z)=-\frac{4\pi i}{\omega}\sigma_l^0(\omega^2-c^2k_\parallel^2)R(k_z)\bar{E}_i^l(k_z)\ , \tag{18}$$

where we have defined another function

$$R(k_z)=R(\mathbf{k}_\parallel,k_z,\omega)\equiv\frac{1}{d}\sum_{G_z}\frac{1}{\omega^2-c^2k_\parallel^2-c^2(k_z+G_z)^2}$$
$$=R(k_z+G_z')\ . \tag{19}$$

This function will play an important role in the subsequent analysis. One can solve (18) to give

$$\bar{E}_i^l(\mathbf{k}_\parallel,k_z,\omega)=\frac{\bar{E}_{\text{ext},i}^l(\mathbf{k}_\parallel,k_z,\omega)}{\epsilon_l(\mathbf{k}_\parallel,k_z,\omega)} \tag{20}$$

where the superlattice longitudinal dielectric function is given by

$$\epsilon_l(\mathbf{k}_\parallel,k_z,\omega)\equiv1+\frac{4\pi i}{\omega}R(k_z)(\omega^2-c^2k_\parallel^2)\sigma_l^0(\mathbf{k}_\parallel,\omega)\ . \tag{21}$$

The zeros of ϵ_l give the longitudinal modes of a superlattice. The fact that $R(k_z)=R(k_z+G_z)$ means that the solutions of (20) and (21) have this same symmetry and thus we can restrict k_z to be in the first Brillouin zone ($0\le k_z\le\pi/d$) of the superlattice. Henceforth, we take $k_z=n\pi/L$ with $n=0,1,\ldots,N-1$ and $L=Nd$. The relation (20) holds for $E_i^l(k_z)$ as well as for $\bar{E}_i^l(k_z)$ defined in (17).

We can discuss the transverse modes in the same way, starting from (16), to obtain

$$\delta\bar{E}_i^t(k_z)=-\frac{4\pi i}{\omega}\sigma_t^0\omega^2R(k_z)\bar{E}_i^t(k_z)\ , \tag{22}$$

where the function $R(k_z)$ has been defined in (19). One

can rewrite (22) in the form

$$\bar{E}_i^t(k_z)=\frac{\bar{E}^t_{\text{ext},i}(k_z)}{D(\mathbf{k}_\parallel,k_z,\omega)} , \tag{23}$$

where the superlattice transverse modes are given by the zeros of

$$D(\mathbf{k}_\parallel,k_z,\omega)=1+4\pi i\omega R(k_z)\sigma_t^0(\mathbf{k}_\parallel,\omega) . \tag{24}$$

The preceding discussion has been concerned with the in-plane electric field components. Inserting (14) into (13), the z component of the electric field is given by

$$\delta E_z(k_z)=\frac{4\pi i}{\omega(\omega^2-c^2k^2)}c^2k_zk_\parallel\bar{E}_\parallel^l(k_z) , \tag{25}$$

where the longitudinal in-plane component $\bar{E}_\parallel^l$ is given by (20) and (21). Clearly the electric field component perpendicular to the metallic sheets is coupled into the longitudinal charge fluctuations described by the zeros of ϵ_l in (21). By the same token, a mode involving a transverse in-phase component $E_\parallel^t$ has *no* associated z component of the electric field.

One may work directly in terms of the longitudinal and transverse components of the superlattice conductivity tensor, which is given by (8). If σ_{ij}^0 is given by (14), one can show that the solutions of (8) are of the form $(i,j=x,y)$

$$\sigma_{ij}(\mathbf{k},-\mathbf{p},\omega)=(2\pi)^2\delta(\mathbf{k}_\parallel-\mathbf{p}_\parallel)\bar{\sigma}_{ij}(\mathbf{k}_\parallel,k_z,\omega)N \times\sum_{G_z}\delta_{p_z,k_z+G_z} , \tag{26}$$

where the reduced in-plane conductivity $\bar{\sigma}_{ij}$ can be decomposed as in (14),

$$\bar{\sigma}_{ij}=\bar{\sigma}_l\hat{k}_i\hat{k}_j+\bar{\sigma}_t(\delta_{ij}-\hat{k}_i\hat{k}_j) . \tag{27}$$

One finds after some calculation that

$$\bar{\sigma}_l(\mathbf{k}_\parallel,k_z,\omega)=\frac{\sigma_l^0(\mathbf{k}_\parallel,\omega)}{\epsilon_l(\mathbf{k}_\parallel,k_z\omega)} , \tag{28a}$$

$$\bar{\sigma}_t(\mathbf{k}_\parallel,k_z,\omega)=\frac{\sigma_t^0(\mathbf{k}_\parallel,\omega)}{D(\mathbf{k}_\parallel,k_z,\omega)} , \tag{28b}$$

where ϵ_l and D are defined in (21) and (24), respectively. Equation (28a) is the generalization of the well known expression for the longitudinal conductivity of a bulk 3D metal (see Chap. 3 of Pines and Nozières[9] as well as Martin[10])

$$\sigma_l(\mathbf{k},\omega)=\frac{\sigma_l^0(\mathbf{k},\omega)}{1+\frac{4\pi i}{\omega}\sigma_l^0(\mathbf{k},\omega)}\equiv\frac{\sigma_l^0(\mathbf{k},\omega)}{\epsilon_l(\mathbf{k},\omega)} \tag{29}$$

to the case of a superlattice of 2D metallic sheets. Similarly, (28b) is the superlattice version of the transverse conductivity of a bulk homogeneous 3D metal

$$\sigma_t(\mathbf{k},\omega)=\frac{\sigma_t^0(\mathbf{k},\omega)}{1+\frac{4\pi i\omega}{\omega^2-c^2k^2}\sigma_t^0(\mathbf{k},\omega)} . \tag{30}$$

We note that it is customary to introduce a transverse dielectric function[9] defined in a manner analogous to ϵ_l in (27),

$$\epsilon_t(\mathbf{k},\omega)\equiv1+\frac{4\pi i}{\omega}\sigma_t^0(\mathbf{k},\omega) . \tag{31}$$

Using this, (30) can be written in an equivalent form which is sometimes used,

$$\sigma_t(\mathbf{k},\omega)=\frac{\sigma_t^0(\omega^2-c^2k^2)}{\omega^2\epsilon_t-c^2k^2} . \tag{32}$$

The free-electron conductivities σ_l^0 and σ_t^0 for a 2D metallic sheet can be easily worked out using (9) and the results given in the Appendix of Harris and Griffin.[12] One finds (for $k_\parallel\ll k_{2F}$)

$$\sigma_l^0(\mathbf{k}_\parallel,\omega)=i\frac{e^2n_0}{m\omega}-i\frac{e^2}{m^2\omega}\int\frac{d\mathbf{p}}{(2\pi)^2}\frac{f(\mathbf{p}+\frac{1}{2}\mathbf{k}_\parallel)-f(\mathbf{p}-\frac{1}{2}\mathbf{k}_\parallel)}{\omega-\frac{pk_\parallel}{m}\cos\theta}p^2\cos^2\theta ,$$

$$\sigma_t^0(\mathbf{k}_\parallel,\omega)=i\frac{e^2n_0}{m\omega}-i\frac{e^2}{m^2\omega}\int\frac{d\mathbf{p}}{(2\pi)^2}\frac{f(\mathbf{p}+\frac{1}{2}\mathbf{k}_\parallel)-f(\mathbf{p}-\frac{1}{2}\mathbf{k}_\parallel)}{\omega-\frac{pk_\parallel}{m}\cos\theta}p^2\sin^2\theta , \tag{33}$$

where $f(\mathbf{p})$ is the Fermi distribution, $\mathbf{p}=(p_x,p_y)$ and we have taken $\mathbf{k}_\parallel$ to be along the x axis ($\mathbf{p}\cdot\mathbf{k}_\parallel=pk_\parallel\cos\theta$). To leading order in $1/\omega$, these general expressions reduce to

$$\sigma_l^0(\mathbf{k}_\parallel,\omega)=\sigma_t^0(\mathbf{k}_\parallel,\omega)=\frac{ie^2n_0}{m\omega}+O\left[\frac{k_\parallel^2}{\omega^3}\right] . \tag{34}$$

For simplicity, we use this in our subsequent evaluation of (21) and (24). It should be adequate for treating the collective modes in a superlattice in the long wavelength limit. For example, Harris and Griffin[12] have shown that the analogous 3D approximation in a film of finite thickness can describe both the bulk and surface plasmon modes, including retardation.

III. SUPERLATTICE PLASMONS WITH RETARDATION

We now discuss the poles of the longitudinal conductivity given by (21). The (retarded) plasmon modes of a superlattice are seen to be given by solutions of

$$1+\frac{4\pi i}{\omega}R(\mathbf{k}_\parallel,k_z,\omega)(\omega^2-c^2k_\parallel^2)\sigma_l^0(\mathbf{k}_\parallel,\omega)=0 \ . \tag{35}$$

Using the long wavelength approximation for σ_l^0 given in (34), this reduces to

$$1=\frac{4\pi n_0 e^2}{m}\left[\frac{\omega^2-c^2k_\parallel^2}{\omega^2}\right]R(\mathbf{k}_\parallel,k_z,\omega) \ . \tag{36}$$

Restricting ourselves to the region $\omega<ck_\parallel$ below the free photon line, one can carry out the reciprocal lattice vector sum in (19) explicitly:[1]

$$R(\mathbf{k}_\parallel,k_z,\omega<ck_\parallel)=-\frac{F_d(\bar{k}_\parallel,k_z)}{2c^2\bar{k}_\parallel} \ , \tag{37}$$

where $\bar{k}_\parallel\equiv\sqrt{k_\parallel^2-(\omega/c)^2}>0$ and

$$F_d(\bar{k}_\parallel,k_z)\equiv\frac{\sinh(\bar{k}_\parallel d)}{\cosh(\bar{k}_\parallel d)-\cos(k_z d)} \ . \tag{38}$$

Inserting (37) into the dispersion relation (36) gives

$$\omega^2=\frac{2\pi n_0 e^2}{m}\bar{k}_\parallel F_d(\bar{k}_\parallel,k_z) \ . \tag{39}$$

This expression was apparently first written down by Fetter.[1] It is equivalent to a zero of the function F in Eq. (30) of Ref. 13. It is also reproduced by the general result given in Eq. (23) of Ref. 5 in the limit of zero external magnetic field (in the notation of Ref. 5, it is equivalent to $S\chi_{yy}+\epsilon_s/2\pi\beta=0$). In the nonretarded limit ($c\to\infty$), $\bar{k}_\parallel$ reduces to $k_\parallel$ and (39) reproduces the well known superlattice plasmon dispersion relation spectrum (see, for example, Refs. 1, 2, and 8).

In the limit of large d (i.e., $\bar{k}_\parallel d\to\infty$), we note that $F_d\to 1$. In this case, (39) reduces to that of a single sheet[14,15]

$$\omega^2=\frac{2\pi n_0 e^2}{m}\bar{k}_\parallel=A\bar{k}_\parallel \ . \tag{40}$$

One can show that $A=v_{2F}^2/a_0$, where $a_0=0.53$ Å is the Bohr radius and v_{2F} is the 2D Fermi velocity. Since $\bar{k}_\parallel$ is a function of ω, the explicit solution of (40) for the 2D plasmon including retardation is the solution of a quadratic equation,

$$\omega^2=\frac{-(A/c)^2+[(A/c)^4+4A^2k_\parallel^2]^{1/2}}{2} \ . \tag{41}$$

There is clearly a crossover wave vector

$$k_\parallel^c\equiv\frac{1}{2}\frac{A}{c^2}=\frac{1}{2a_0}\left[\frac{v_{2F}^2}{c^2}\right] \tag{42}$$

such that for $k_\parallel<k_\parallel^c$, the solution of (41) approaches the free photon dispersion relation $\omega=ck_\parallel$ (see Sec. VI of Ref. 14 as well as Ref. 15). For $k_\parallel\gg k_\parallel^c$, the 2D plasmon goes over to the usual nonretarded expression in (1).

Since this does not seem to be given in the literature, we briefly discuss the retarded solutions of (39) in the opposite limit of small d. In this case, (38) reduces to

$$F_d(\bar{k}_\parallel,k_z)\simeq\frac{1}{d}\frac{2\bar{k}_\parallel}{\bar{k}_\parallel^2+k_z^2} \ . \tag{43}$$

In this case ($\bar{k}_\parallel d,k_z d\ll 1$), the superlattice plasmon spectrum (39) is given by (see also Ref. 8)

$$\omega^2=\omega_B^2\frac{\bar{k}_\parallel^2}{\bar{k}_\parallel^2+k_z^2} \ , \tag{44}$$

where the superlattice plasmon frequency is defined as

$$\omega_B^2=\frac{4\pi n_B e^2}{m} \ , \tag{45}$$

and $n_B=n^0/d$ is the effective bulk electronic density. The $k_z=0$ mode is a special case and is discussed in Sec. V. For $k_z\neq 0$, the plasmon modes predicted by (44) have an acoustic dispersion relation for sufficiently small values of $\bar{k}_\parallel\ll k_z$, namely

$$\omega=\frac{\omega_B}{k_z}\bar{k}_\parallel(\omega) \ . \tag{46a}$$

One may easily solve (46a) to obtain ($k_z\neq 0$)

$$\omega^2=\frac{s^2k_\parallel^2}{1+\frac{s^2}{c^2}}; \quad s\equiv\frac{\omega_B}{k_z} \ . \tag{46b}$$

This is illustrated in Fig. 1. For $s\gg c$, these solutions approach $\omega=ck_\parallel$ from below. For $s\ll c$, we have the (nonretarded) result $\omega=sk_\parallel$.

IV. TRANSVERSE EM MODES IN A SUPERLATTICE

According to (24), the transverse modes in a superlattice are given by the solutions of

$$1+\frac{4\pi i}{\omega}R(\mathbf{k}_\parallel,k_z,\omega)\omega^2\sigma_t^0(\mathbf{k}_\parallel,\omega)=0 \ . \tag{47}$$

The same dispersion relation is reproduced by Eq. (23) of Ref. 5 in the limit of zero external magnetic field (in the notation of Ref. 5, it is equivalent to $S\chi_{xx}-\beta c^2/2\pi\omega^2=0$). Using (34), this reduces to [compare with the longitudinal result in (36)]

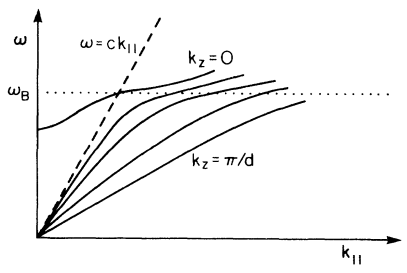

FIG. 1. Sketch of the superlattice longitudinal plasmon dispersion relation for various values of k_z. For small $k_\parallel$, the $k_z\neq 0$ results are given by (46b). The $k_z=0$ plasmon mode is discussed in Sec. V.

$$1=\frac{4\pi n_0 e^2}{m}R(\mathbf{k}_\parallel,k_z,\omega)\ . \tag{48}$$

This dispersion relation is given by $F'=0$, where F' is defined in Eq. (31) of Ref. 13. It is clear from (37) that there are *no* real solutions of (48) in the region $\omega<ck_\parallel$ since $R<0$. We thus restrict our attention to $\omega>ck_\parallel$.

We first consider (48) in the limit of small separation $d\to 0$. In this limit, only the $G_z=0$ term contributes to the sum in (19) and thus we are left with

$$R(\mathbf{k}_\parallel,k_z,\omega)=\frac{1}{d(\omega^2-c^2k_\parallel^2-c^2k_z^2)}\ . \tag{49}$$

Putting this into (48) gives the usual transverse mode dispersion relation of a 3D metal,

$$\omega^2=\omega_B^2+c^2(k_\parallel^2+k_z^2)\ , \tag{50}$$

where in this limit k_z may be viewed as a continuous variable.

In the opposite limit of a large separation distance ($d\to\infty$), the G_z sum can be transformed into a contour integral which can be evaluated explicitly:

$$R(\mathbf{k}_\parallel,k_z,\omega>ck_\parallel)=\frac{1}{c^2}\int_{-\infty}^{\infty}\frac{dp_z}{2\pi}\frac{1}{K^2-p_z^2}$$

$$=\frac{i}{2Kc^2}\ , \tag{51}$$

where we have defined

$$K^2\equiv(\omega/c)^2-k_\parallel^2>0\ . \tag{52}$$

Inserting (51) into (48), we see that there are no real solutions in the $d\to\infty$ limit. That is, there are no transverse EM waves associated with a single 2D metallic sheet, with the electric field in the plane of the sheet.

We note that for $\omega>ck_\parallel$, the function $R(k_z)$ in (19) has poles whenever $K=k_z+G_z$ and hence (48) has multiple solutions (see Fig. 2). However, since $R(k_z)=R(k_z+G_z)$, we need only consider the lowest solution in the first Brillouin zone.

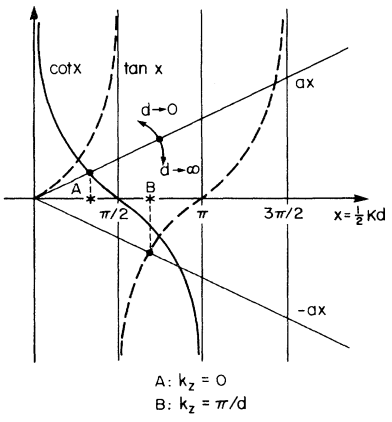

FIG. 2. Graphical solution (schematic) for the transverse mode solutions for $k_z=0$ [see (55)] and $k_z=\pi/d$ [see (59)].

For $K^2>0$, one can carry out the sum in (19) explicitly using the general formula (q real)

$$\frac{1}{id}\sum_{G_z}\frac{1}{G_z+q}=\frac{1}{e^{iqd}-1} \tag{53}$$

to give

$$R(\mathbf{k}_\parallel,k_z,\omega>ck_\parallel)=-\frac{1}{2Kc^2}\frac{\sin(Kd)}{\cos(Kd)-\cos(k_zd)}\ . \tag{54}$$

We now turn to a detailed discussion of the transverse mode dispersion relation at both $k_z=0$ and $k_z=\pi/d$, the boundaries of the first Brillouin zone (BZ) of the superlattice. For $k_z=0$, (54) reduces to $R(\mathbf{k}_\parallel,k_z=0,\omega>ck_\parallel)=(1/2Kc^2)\cot\frac{1}{2}Kd$. Inserting this into (48), the transverse EM modes for $k_z=0$ are given by the lowest energy solution $x\equiv\frac{1}{2}Kd$ of

$$\cot x=ax;\quad a\equiv\frac{c^2}{\frac{\pi n_0e^2d}{m}}=2\frac{c^2}{v_{2F}^2}\left[\frac{a_0}{d}\right]\ . \tag{55}$$

The last expression for a follows from the result given just below (40). Except in the limit of extremely large d, we note that the slope a is always much larger than unity. The graphical solution of (55) is shown in Fig. 2 (denoted as A).

If we denote the solution of (55) as x^* for a given value of d, the $k_\parallel$ dependence of the $k_z=0$ transverse mode is then given by

$$\omega^2(\mathbf{k}_\parallel,k_z=0)=c^2\left[\frac{2x^*}{d}\right]^2+c^2k_\parallel^2\ . \tag{56}$$

For $d\to 0$, we can approximate $\cot x\simeq 1/x$ and the solution of (55) is

$$x^*=\frac{1}{\sqrt{a}}\quad\text{or}\quad\omega=\omega_B\quad\text{at}\quad k_\parallel=0\ , \tag{57}$$

which is equivalent to the result $\omega^2=\omega_B^2+c^2k_\parallel^2$ given in (50). More generally, we see that the slope a decreases as d increases, with the limiting solution given by $x=\pi/2$. In particular, we conclude that for $k_\parallel=0$, the $k_z=0$ transverse mode frequency is given by

$$\omega(\mathbf{k}_\parallel=0,k_z=0)\geq\omega_B\quad\text{for } d\to 0\ ,$$
$$\omega(\mathbf{k}_\parallel=0,k_z=0)\leq\frac{\pi c}{d}\quad\text{for } d\to\infty\ . \tag{58}$$

This means that while the frequency increases with d, at a sufficiently large value of d, it must start to decrease. However the large d limit is singular in that there is no transverse mode when $d=\infty$. This is consistent with our previous null result for a single 2D sheet.

The other boundary of the first BZ corresponds to $k_z=\pi/d$, with charge fluctuations in alternate sheets being out of phase.[1] In this case, (54) reduces to $R(\mathbf{k}_\parallel,k_z=\pi/d,\omega>ck_\parallel)=-(1/2Kc^2)\tan(\frac{1}{2}Kd)$. Inserting this into (48), the $k_z=\pi/d$ transverse modes are seen to be given by the solutions of

$$\tan x = -ax \ , \tag{59}$$

in place of (55). The graphical solution giving $x = \frac{1}{2}Kd$ is also sketched in Fig. 2 (denoted as B). The solutions clearly lie in the range $\pi/2 \leq x \leq \pi$ as d varies.

Summarizing our results so far concerning the transverse mode solutions of (48), we see from Fig. 2 that for a given value of the separation distance d, we have a band of frequencies of finite width $0 < K < 2\pi/d$ corresponding to the N values of $k_z (0 \leq k_z \leq \pi/d)$. As d becomes large, this bandwidth clearly narrows to zero. This is expected since the coupling between the layers is weakening as d increases. In the limit of $d \to \infty$, the bandwidth vanishes. In fact, as noted above this case reduces to an isolated 2D sheet described by (51), which does not sustain any transverse EM modes (for a sheet of finite thickness, see Ref. 16). In the opposite limit, as d becomes smaller, the bandwidth widens, reflecting the increased coupling of the different superlattice layers. In Fig. 3, we sketch the spectrum of the $k_z = 0$ transverse EM modes for various values of the superlattice period d. At $k_\parallel = 0$, these frequencies can be shown to be degenerate with the $k_z = 0$ longitudinal plasmons (see Sec. V).

V. THE $k_z = 0$ LONGITUDINAL PLASMON

We are now in a position to consider the $k_z = 0$ longitudinal plasmon mode. The $k_z \neq 0$ modes, discussed in Sec. III, only occur in the region $\omega < ck_\parallel$. In contrast, we find there is a $k_z = 0$ solution of (36) in the region $\omega > ck_\parallel$ as well as $\omega < ck_\parallel$. We recall[1] that the $k_z = 0$ plasmon corresponds to all sheets in a superlattice oscillating in phase.

We first consider the region $\omega < ck_\parallel$. In this case, $F_d(\bar{k}_\parallel, k_z = 0)$ in (38) reduces to $\coth \frac{1}{2}\bar{k}_\parallel d$ and then (39) can be conveniently rewritten in the form

$$\tanh x = \frac{\omega_B^2}{\omega^2} x; \quad x \equiv \tfrac{1}{2}\bar{k}_\parallel d \ . \tag{60}$$

One easily sees that it only has a solution if $\omega > \omega_B$ [and of course (39) and (60) are only valid for $\omega < ck_\parallel$]. As ω decreases towards ω_B, the solution of (60) is given by

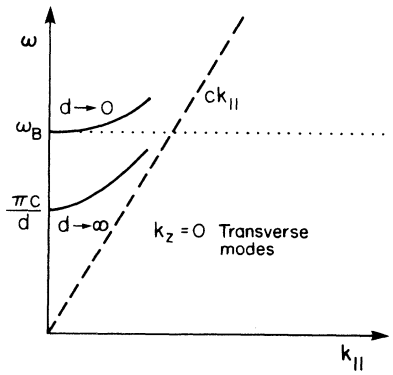

FIG. 3. Sketch of the $k_z = 0$ transverse EM mode spectrum as a function of the superlattice spacing d. Initially the frequency increases with d but for large enough values of d, it starts to decrease.

$x \to 0$ or $\bar{k}_\parallel \to 0$. We conclude that for $k_z = 0$, the longitudinal plasmon frequency intersects the $\omega = ck_\parallel$ line at $\omega = \omega_B$. This qualitatively different behavior of the $k_z = 0$ and $k_z \neq 0$ solutions of (39) shown in Fig. 1 also occurs in the nonretarded limit ($c \to \infty$ or $\bar{k}_\parallel = k_\parallel$). In the opposite limit $\omega \gg \omega_B$, the solution of (60) clearly corresponds to $(\omega_B/\omega)^2 x = 1$, which reduces to the 2D plasmon result in (40).

We next discuss the continuation of the $k_z = 0$ plasmon given by (60) into the region $\omega > ck_\parallel$. In this region, the solution of (36) involves the R function given in (54). The dispersion relation (36) can be conveniently rewritten in the form

$$\tan y = \frac{\omega_B^2}{\omega^2} y; \quad y \equiv \tfrac{1}{2}Kd \ . \tag{61}$$

A solution of (61) immediately shows that the only solutions are in the region $\omega \leq \omega_B$ (and also $\omega > ck_\parallel$). As with (60), one sees that the mode intersects $\omega = ck_\parallel$ ($y = 0$) at $\omega = \omega_B$. As $k_\parallel$ decreases, the solution decreases in frequency but with y increasing towards $y = \pi/2$.

The solution at $k_\parallel = 0$ is especially simple. We note that (36) becomes identical to (48) at $k_\parallel = 0$, for any value of k_z [recall that Eq. (34) is exact at $k_\parallel = 0$]. However, the only solutions of (48) are in the region $\omega > ck_\parallel$ and moreover all solutions of (36) are in the region $\omega < ck_\parallel$ for $k_z \neq 0$. Thus it is only the $k_z = 0$ longitudinal plasmon which becomes degenerate with the $k_z = 0$ transverse mode at $k_\parallel = 0$. This longitudinal frequency spectrum at $k_\parallel = 0$ is bounded as in (58) and is shown in Fig. 3.

We have shown explicitly that at $\mathbf{k}_\parallel = \mathbf{0}$, the $k_z = 0$ longitudinal and transverse EM modes in a superlattice are degenerate. A similar degeneracy at $\mathbf{k} = \mathbf{0}$ is well known[9] in a 3D bulk metal [see Eq. (2)]. Both results are expected, being a consequence of the fact that the transverse and longitudinal response of any charged system must be identical when the wavelength of the probe is much larger than any spatial inhomogeneity and other characteristic lengths.

VI. CONCLUDING REMARKS

We have developed a general procedure for studying the EM modes of layered electronic structures, based on (7) and (8). We have illustrated our approach by working out the modes in a simple superlattice described by (10). In this case, (7) reduces to (12) and (13). The dispersion relations for longitudinal and transverse EM modes were found to be given by (35) and (47), respectively. These are equivalent to the results obtained by different methods in Refs. 5, 6, and 13.

In our detailed analysis of the dispersion relation of the superlattice modes in Secs. III–V, we limited ourselves to the long wavelength description of the metallic sheets, as described by (34). It is straightforward to work out the next order corrections using the results given by (A8) in the Appendix for $\sigma^0_{l,t}(\mathbf{k},\omega)$ for a 2D electron gas.

This work has been motivated by the metallic superlattice structure exhibited by the high-T_c superconductors.[8]

In fact, in the oxide superconductors, one is dealing with superlattices with a unit cell of up to three closely spaced metallic sheets (which may not have the same electronic structure). One can easily extend our present analysis to these more complicated structures (see Ref. 8). The case of a single bilayer is of special interest. In this case, the electronic density is described by

$$n_0(\mathbf{r})=n_0[\delta(z)+\delta(z-d)] \tag{62}$$

instead of the periodic structure in (10). In place of (12), we obtain ($i=x,y$)

$$\delta E_i(\mathbf{k}_\parallel,k_z)=\frac{4\pi i}{\omega(\omega^2-c^2k^2)}\sum_{n,m=x,y}(c^2k_ik_n-\omega^2\delta_{in})\sigma^0_{nm}(\mathbf{k}_\parallel,\omega)(1+e^{id(k_z-p_z)}]E_m(\mathbf{k}_\parallel,p_z)\ . \tag{63}$$

It is straightforward to solve (63) for the longitudinal plasmons in such a bilayer. After a certain amount of algebra one finds for $\omega<ck_\parallel$ that there are two solutions

$$\omega_\pm^2=\frac{2\pi n_0e^2}{m}\bar{k}_\parallel(1\pm e^{-\bar{k}_\parallel d})\ , \tag{64}$$

where $\bar{k}_\parallel\equiv[k_\parallel^2-(\omega/c)^2]^{1/2}$ and for simplicity we again have used (34) for $\sigma_l^0(\mathbf{k}_\parallel,\omega)$. These two modes are the natural generalization of the nonretarded calculation ($\bar{k}_\parallel\to k_\parallel$) and describe the high energy in-phase (ω_+) and low energy out-of-phase (ω_-) charge oscillations in the two coupled sheets.[17,8] For $\bar{k}_\parallel d\ll 1$, we find

$$\omega_-^2=\frac{\dfrac{2\pi n_0e^2d}{m}k_\parallel^2}{1+\dfrac{2\pi n_0e^2d}{\pi}\dfrac{1}{c^2}}\ . \tag{65}$$

The velocity approaches c as d becomes very large (i.e., when $d>a_0c^2/v_{2F}^2$).

ACKNOWLEDGMENTS

This work was supported by an operating grant from NSERC of Canada. H.S. also wishes to thank the Run Run Shaw Foundation, Hong Kong.

APPENDIX

For completeness as well as future work, we give an expanded discussion of (33) quoted in the text. In a 2D electron gas, (9) reduces to ($i,j=x,y$)

$$\sigma^0_{ij}(\mathbf{k}_\parallel,\omega)=\frac{ie^2n_0}{m\omega}\delta_{ij}+\frac{e^2}{i\omega}\chi^0_{ij}(\mathbf{k}_\parallel,\omega)\ , \tag{A1}$$

where the 2D free-electron current-current response function is

$$\chi^0_{ij}(\mathbf{k}_\parallel,\omega)=2\int\frac{d\mathbf{p}}{(2\pi)^2}\times\frac{f(\mathbf{p}+\frac{1}{2}\mathbf{k}_\parallel)-f(\mathbf{p}-\frac{1}{2}\mathbf{k}_\parallel)}{\omega-\dfrac{\mathbf{p}\cdot\mathbf{k}_\parallel}{m}}\left[\frac{p_i}{m}\right]\left[\frac{p_j}{m}\right] \tag{A2}$$

in the long wavelength limit ($k_\parallel\ll k_{2F}$). The spin degeneracy factor has been included.

One can easily see that $\chi^0_{ij}=0$ for $i\neq j$. Combining (A1) with (14), one obtains ($\hat{k}_i=k_i/k_\parallel$)

$$\sigma_l^0(\mathbf{k}_\parallel,\omega)=i\frac{e^2n_0}{m\omega}-\frac{ie^2}{\omega}(\hat{k}_x^2\chi^0_{xx}+\hat{k}_y^2\chi^0_{yy})\ , \tag{A3}$$

$$\sigma_t^0(\mathbf{k}_\parallel,\omega)=i\frac{e^2n_0}{m\omega}-\frac{ie^2}{\omega}(\hat{k}_x^2\chi^0_{yy}+\hat{k}_y^2\chi^0_{xx})\ , \tag{A4}$$

These results lead directly to (33). We note that the continuity equation implies that

$$\sum_{ij}\hat{k}_i\chi^0_{ij}\hat{k}_j=\frac{\omega^2}{k_\parallel^2}\chi^0_{nn}+\frac{n_0}{m}\ , \tag{A5}$$

where χ^0_{nn} is the 2D free-electron density response function (Lindhard function).

The expressions in (33) can be evaluated analytically up to terms of order $k_\parallel^4$ at $T=0$ and we obtain ($A\equiv\omega/v_{2F}k_\parallel$)

$$\sigma_l^0(\mathbf{k}_\parallel,\omega)=\begin{cases}-\dfrac{2ie^2n_0}{m\omega}A^2\left[1-\dfrac{A}{\sqrt{A^2-1}}\right], & A>1\ ,\\ -\dfrac{2ie^2n_0}{m\omega}A^2\left[1+\dfrac{iA}{\sqrt{1-A^2}}\right], & A<1\ ,\end{cases} \tag{A6}$$

$$\sigma_t^0(\mathbf{k}_\parallel,\omega)=\begin{cases}\dfrac{2ie^2n_0}{m\omega}\left[A^2+(1-A^2)\dfrac{A}{\sqrt{A^2-1}}\right], & A>1\ ,\\ \dfrac{2ie^2n_0}{m\omega}\left[A^2-(1-A^2)\dfrac{iA}{\sqrt{1-A^2}}\right], & A<1\ .\end{cases} \tag{A7}$$

In the long wavelength limit $A\gg 1$, the lowest order corrections to (34) are easily found:

$$\sigma_l^0(\mathbf{k}_\parallel,\omega)=\frac{ie^2n_0}{m\omega}\left[1+\frac{3}{4}\frac{1}{A^2}+\cdots\right]\ ,$$
$$\sigma_t^0(\mathbf{k}_\parallel,\omega)=\frac{ie^2n_0}{m\omega}\left[1+\frac{1}{4}\frac{1}{A^2}+\cdots\right]\ . \tag{A8}$$

Finally we note that combining (A5) with (A6) gives the 2D Lindhard function[15,8]

$$\chi^0_{nn}(\mathbf{k}_\parallel,\omega)=N(\varepsilon_F)\left[1-\frac{A}{\sqrt{A^2-1}}\right],\quad A>1\ , \tag{A9}$$

where $N(\varepsilon_F)=m/\pi$ is the density of states at the Fermi surface.

[1]A. L. Fetter, Ann. Phys. (N.Y.) **88**, 1 (1974).
[2]S. Das Sarma and J. J. Quinn, Phys. Rev. B **25**, 7603 (1982).
[3]J. K. Jain and S. Das Sarma, Surf. Sci. **196**, 466 (1988).
[4]A. C. Tselis, G. Gonzalez de la Cruz, and J. J. Quinn, Solid State Commun. **47**, 43 (1983).
[5]A. C. Tselis and J. J. Quinn, Phys. Rev. B **29**, 2021 (1984).
[6]R. D. King-Smith and J. C. Inkson, Phys. Rev. B **36**, 4796 (1987).
[7]W. L. Mochán and M. del Castillo-Mussot, Phys. Rev. B **37**, 6763 (1988).
[8]A. Griffin and A. J. Pindor, Phys. Rev. B **39**, 11 503 (1989).
[9]D. Pines and P. Nozières, *The Theory of Quantum Liquids* (Benjamin, New York, 1966), Vol. I.
[10]P. C. Martin, Phys. Rev. **161**, 143 (1967).
[11]K. W. Chiu and J. J. Quinn, Phys. Rev. B **9**, 4724 (1974).
[12]J. Harris and A. Griffin, Phys. Rev. **3**, 749 (1971).
[13]M. Babiker, N. C. Constantinou, and M. G. Cottam, J. Phys. C **19**, 5849 (1986).
[14]A. L. Fetter, Ann. Phys. (N.Y.) **81**, 376 (1973).
[15]F. Stern, Phys. Rev. Lett. **18**, 546 (1967).
[16]D. A. Dahl and L. J. Sham, Phys. Rev. B **16**, 651 (1977).
[17]See, for example, G. F. Santoro and G. F. Giuliani, Phys. Rev. B **37**, 937 (1988).